LASER-MICROMACHINED PERMANENT MAGNET ARRAYS WITH SPATIALLY ALTERNATING MAGNETIC FIELD DISTRIBUTION

B.A. Peterson[1]*, W.C. Patterson[2], F. Herrault[1], D.P. Arnold[2], and M.G. Allen[1]
[1]Electrical and Computer Engineering, Georgia Institute of Technology, Atlanta, GA, USA
[2]Interdisciplinary Microsystems Group, Electrical and Computer Engineering, University of Florida, Gainesville, FL, USA

Abstract: Many MEMS systems can benefit from dense, alternating arrays of permanent magnets (PM) with high energy-product and substantial magnetic flux density adjacent to the array. In this work, we demonstrate laser machining fabrication and assembly techniques to create linear PM alternating arrays with periods as low as 230 µm. Comb-shaped magnet structures are micromachined from a 300 µm thick samarium cobalt (SmCo) substrate using an IR laser. These structures are then magnetized and assembled in an interlocking fashion to make alternating magnet arrays of various total lengths. Scanning Hall-effect sensor measurements taken 80 µm above the surface indicate sinusoidally varying magnetic fields with periods as expected from the underlying magnet geometry and peak magnetic flux density amplitudes of 0.1 T.

Keywords: laser microfabrication, permanent magnet, magnet array, micromagnet

INTRODUCTION

Permanent magnets have the potential to play a useful role in many microelectromechanical systems (MEMS) including micromotors, microgenerators, energy harvesters, magnetic actuators, undulators, and travelling wave tubes [1,2,3]. However, there are a number of obstacles to the integration of permanent magnets (PM) with MEMS, including the need for very high temperature treatment of typical bulk magnetic materials to produce the highest energy-product magnets. Although there have been a number of MEMS-based approaches to integrate non-bulk magnets, obtaining both a high energy product and the large magnet thickness required to sustain the magnetic field at larger physical distances from the magnet has been challenging.

In addition to the integration of magnets themselves, there has been an increasing research effort towards creating MEMS-scale multi-pole PM arrays. Such multipole arrays are typically both spatially dense and alternately-poled, i.e., a magnetic north pole in close proximity to a magnetic south pole (Fig. 1). A number of key parameters can be used to assess the quality of these arrays, including the spatial density or pole width; the width of the transition region or dead zone (if any) between the individual poles; and the strength of the array magnetic field generated at some scaled distance from the array. Techniques such as magnetic patterning of bulk commercially-available SmCo and NdFeB continuous films using pulsed magnetization techniques have been reported [2,3] and demonstrated mm-scale pole pitches. Using a combination of laser micromachining and manual assembly, mm-scale PM array for magnetic rotors were demonstrated [4]. At smaller magnet thickness scales, thermomagnetically-patterned sputtered NdFeB films have also been presented and exhibited alternating magnetic field distribution with a magnetization reversal technology based on localized laser-induced heating under externally-applied magnetic field [5]. Topographically-patterned PM films, which consisted of sputtered PM material onto microstructured silicon substrates, also exhibited multi-pole magnetization, and periods smaller than 100 µm were demonstrated with film thicknesses on the order of 40 µm [6]. More recently, it was reported that arrays exhibited alternating magnetic field distribution by appropriately spacing uniformly axially-magnetized magnets. The PM arrays were microfabricated NdFeB with 300-µm pole width and 300-µm-wide spacing [7]. Although not fabricated using MEMS technologies, a cm-scale Halbach array, a particular magnet configuration to create multi-pole arrays, was assembled for use in energy harvester applications [8].

We recently reported that laser micromachining technology enabled the fabrication of high-aspect-ratio SmCo and NdFeB micromagnets [9]. PM microstructures as small as 50-µm-wide and 300-µm-thick were microfabricated, and exhibited 80% of the bulk material magnetization, indicating minimal laser damage. Since this approach is based on the bulk machining of magnetic material, it may be possible to maintain the high bulk material energy-product rather than trying to replicate it through MEMS processes.

This paper focuses on the fabrication and assembly methodologies to create multi-pole PM arrays using

this laser micromachining technology, with an emphasis on decreasing the array period (or pole pitch) while maintaining large alternating magnetic field intensities. An illustration of these PM arrays with sub-mm-scale period is shown in Fig. 1, and features interdigitated microstructures with alternating magnetization. Magnetic modeling of such arrays is performed to assess the magnetic field intensity generated by these arrays. Magnetic field measurements are also reported and discussed.

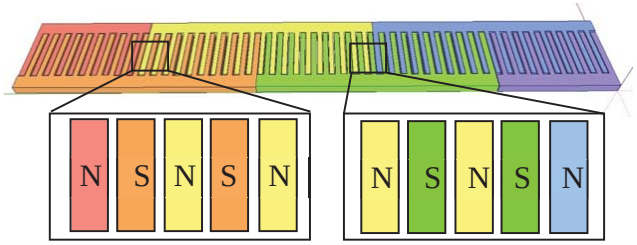

Fig. 1: Conceptual rendering of a PM array with spatially alternating magnetic field distribution.

DESIGN CONSIDERATIONS

As mentioned above, key performance criteria for the design of permanent magnet arrays include the spatial density (i.e., period) and the magnetic flux density at some scaled orthogonal distance from the array (where scaled distance refers to the distance from the array relative to the array period).

As discussed above, our approach to fabricating micromagnets involves laser micromachining bulk rare-earth magnet substrates. As the physical size of the magnets shrinks, nonuniformities in the laser removal process, and the resultant gap tolerance from magnet-to-magnet, may result in a gap that is a significant fraction of the total period. Even if the physical gap between magnets can be minimized, it is possible that the laser machining process may induce a 'damage zone' that would render a portion of the magnet, which had been exposed by the cutting action of the laser beam, to be ineffective. It has been demonstrated phenomenologically that this zone of damaged material propagates only approximately ten microns from the laser-cut magnet edge into the bulk of the magnet [5]. This damage zone, together with the physical gap required for accommodation of assembly tolerance, may result in inefficiencies and/or nonidealities in the array performance.

In order to assess the potential magnitude of this effect, a COMSOL Multiphysics simulation was performed in which the effect of progressively increasing dead zones on the magnetic flux density of the array at a fixed distance from the array is assessed. Referring to the upper portion of Fig. 2, consider three nominal cases: a magnetic array with spatial period of 400 µm, comprising vertically poled north and south segments with 1) no dead zone, and dead zones of 2) 40%, and 3) 70%. COMSOL is used to calculate the z-component of the spatially varying magnetic flux density at 80 µm from the surface of the array with varying dead zone percentages. The ratio of the magnetic flux density of a given percentage loss of material to that of the nominal (lossless) case is plotted as a function of the percentage of material loss (i.e., dead zone extent) in the lower portion of Fig. 2. As can be seen, 80% of the nominal value of flux density at a given lateral point at a height of 80 µm above the array surface can be maintained even with 40% of the array magnetic material being removed or ineffective. This result suggests that for these geometries, efforts to maximize the nominal magnetic flux density of the material may be more effective in maintaining significant magnetic flux densities at some distance from the array than minimizing the material loss between array elements.

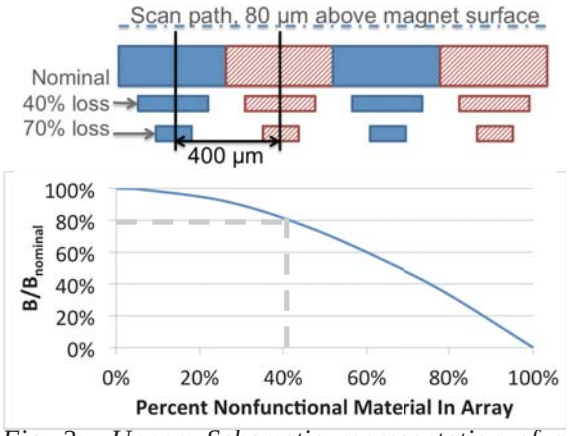

Fig. 2: Upper: Schematic representation of an alternating magnet array illustrating cases with progressively more nonfunctional material comprising the array. Lower: plot of flux density 80 microns above the array surface as a function of nonfunctional material comprising the array.

FABRICATION AND ASSEMBLY

To demonstrate our methodology to create multi-pole PM arrays with sub-mm-scale pole pitch, 300-µm-thick Sm_2Co_{17} material was selected because it exhibits high energy-product (30 MGOe), high remanence (1.1 T), and high coercivity (9 kOe) (Pacific PAC Technologies, Inc.). Further, we previously demonstrated that this material was compatible with laser micromachining, both from structural and magnetic characteristics [1,9]. The demagnetized SmCo microstructures were fabricated using an infrared Nd:YLF laser (Resonetics) with a pulse width of 100 µs, a 1 kHz pulse frequency and a cut speed of 30 µm/s.

Laser-micromachined SmCo microstructures are shown in Fig. 3, and consist of arrays of ten 1-mm-long permanent-magnet beams. Figure 3(a) shows an array with 80-µm-wide magnets and a corresponding pole pitch of 250 µm, while Fig. 3(b) depicts a similar array with 60-µm-wide magnets and a 230-µm-long period. Because the complementary array cut out is re-used to reform the PM array after magnetization, the pole pitch is typically larger than two pole widths due to the material removed by laser micromachining. In order to remove laser-induced material debris, the comb-shaped microstructures were cleaned in 15% citric acid solution heated at 80ºC. A chemically-vapor-deposited film of parylene was subsequently deposited onto the PM arrays. This protective layer acted as a packaging material to reduce oxidation and physical damage.

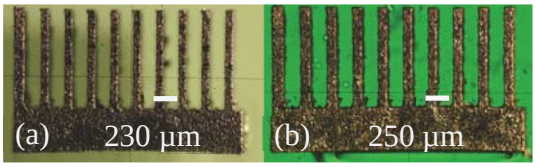

Fig. 3: Photographs of (a) a 10-period comb after laser machining with a period of 250 µm and (b) a similar 10-period comb with 230-µm-long period.

After laser fabrication and parylene coating, the individual PM microstructures were magnetized in the thickness direction using a 7 T superconducting magnet (Bruker DSX 300), ensuring full magnetization. The comb-shaped PM arrays were subsequently assembled by sliding one array into its complementary mate (Fig. 4). A photograph of a 20-mm-long assembled PM array with 50 periods of 400 µm is shown in Fig. 5. For characterization, the PM array was inserted into a non-magnetic aluminum frame and affixed using epoxy. After assembly, the sample was polished to achieve a uniform surface and coated with a thin layer of parylene. This multi-pole PM array was assembled using the interlocking approach presented in Fig. 4, demonstrating cm-scale arrays with sub-mm-scale magnet registration.

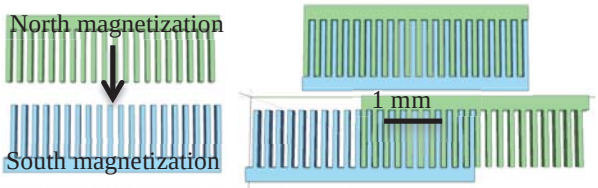

Fig. 4: Schematic of assembly methods: Two combs are laser micromachined and separated from each other. (right) Two assembly methods: (top) a single PM array, and (bottom) interlocking array allowing longer arrays with additional combs.

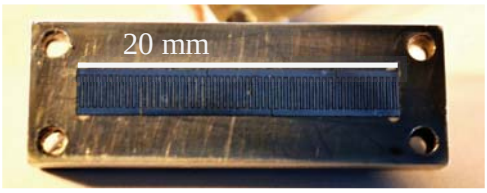

Fig. 5: Photograph of an assembled and polished magnet array with 50 magnetic periods of 400 µm. The active area is 2 mm wide by 20 mm long.

RESULTS

After assembly, the PM arrays were characterized using a Hall-effect sensor experimental setup. The test setup consisted of a computer-controlled stage with *x-y-z* micropositioners and a Hall sensor (1 µm x 1 µm active area, NanoMagnetics Instruments, Inc.). The arrays were magnetically scanned with a step size of 10 µm. Figure 6 shows an experimentally measured magnetic map of a section of the PM array shown in Fig. 5. The centerline, which is defined as the line along the x-axis that crosses the center of the interdigitated fingers (i.e., at y = 1.25 mm for this specific map), shows a symmetric and alternating magnetic field distribution. A magnetic field gradient along each individual finger was also observed. This effect, which was predicted by simulation, was caused by the magnetized sidebars that were used to maintain structural integrity of the comb-like microstructures.

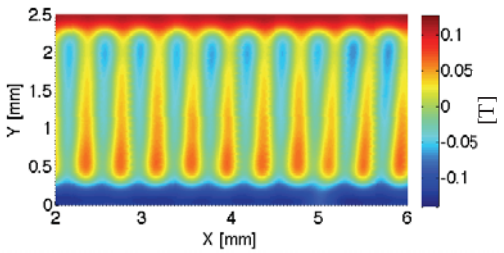

Fig. 6: Magnetic map of a section of the 400-µm-period PM array shown in Figure 5. The magnetic field intensity was measured at 100 µm above the array surface, and the scale is in Tesla.

Figure 7 shows a 1-D plot of the magnetic field measured along the centerline of the PM array with a 300-µm-long period at various sensor heights (namely, 80, 100 and 150 µm above the array surface). These measurements are in good agreement with the simulated results. For measurements performed at 80 µm above the PM array surface, the peak-to-peak magnetic field intensity was measured at 0.20 T with a standard deviation of approximately 0.02 T. Further, the measured magnetic period exhibited a 2% standard deviation from the designed 300-µm-long period. These quantitative measurements successfully validate the fabrication

and assembly approaches utilized to create multi-pole PM arrays with sub-mm-scale periods.

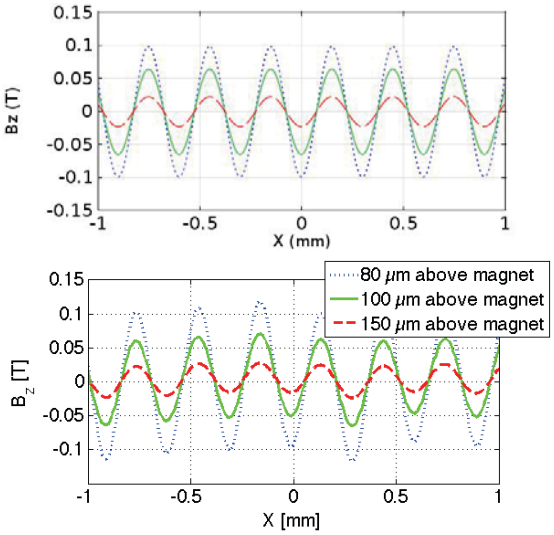

Fig. 7: COMSOL simulations (upper) and respective magnetic field measurements (lower) along the centerline of a 300-µm-period PM array at various heights (80, 100 and 150 µm).

The experimental results obtained for the finer PM arrays with pole pitches designed at 230 and 250 µm, are plotted in Fig. 8. As the pole pitch of PM arrays decreases, the percentage of removed material between poles caused by the laser micromachining becomes more significant. For these arrays, approximately 40-50% of the magnetic material was removed. In spite of this current fabrication limitation, the arrays still exhibit peak magnetic field intensities of approximately 0.06 T.

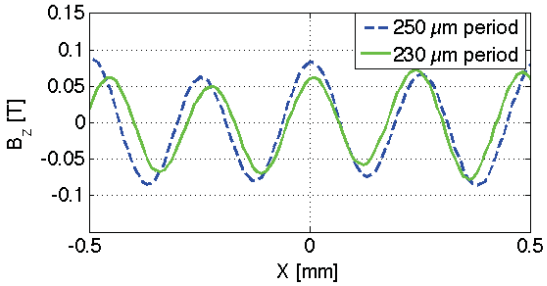

Fig. 8: Magnetic field measurements along the centerline of two distinct PM arrays with period widths at 250 µm (blue, dashed) and (green, solid) 230 µm. The field intensity was measured at 80 µm above the array surface.

CONCLUSION

This work demonstrates the fabrication and assembly of 300-µm-thick SmCo PM arrays with pole pitches ranging from 230 to 400 µm and exhibiting alternating magnetic field patterns. Using a Hall-sensor-based magnetic scanner, magnetic fields generated from these arrays were measured, and intensities higher than 0.1 T were recorded at 80 µm from the magnet array surface. These results are particularly attractive for permanent-magnet-based MEMS devices that often require high magnetic field intensities and fine pole pitches, such as magnetic micro-actuators, micro-harvesters, micro-generators, or micro-undulators.

ACKNOWLEDGEMENTS

This work was supported in part by the DARPA AXiS program under grant #N6601-11-1-4198.

REFERENCES

[1] Arnold D.P. and Wang N., Permanent Magnets for MEMS *J. Microelectromech. Syst.*, **18** 1255-66

[2] Topfer J. and Christoph V., Multi-pole Magnetization of NdFeB Sintered Magnets and Thick Films for Magnetic Micro-Actuators, *Sensors and Actuators A*, **113**257-64

[3] Zana I., Herrault F., Arnold D.P., and Allen M.G., Magnetic Patterning of Permanent-Magnet Rotors for Microscale Motor/Generators, *PowerMEMS 2005, (Tokyo, Japan, 28-30 November 2005)* 116-119

[4] Herrault F., Ji C.-H., and Allen M.G., Ultraminiaturized, High-Speed, Permanent-Magnet Generators for Milliwatt-Level Power Generation, *J. Microelectromech. Syst.*, **17** 1376-87

[5] Dumas-Bouchiat F., *et al.*, Thermomagnetically patterned micromagnets, *Appl. Phys. Letters*, **96** 102511-4

[6] Kustov M., *et al..*, Magnetic Characterization of Micropatterned Nd-Fe-B Hard Magnetic Films Using Scanning Hall Probe Microscopy, *J. of Applied Physics*, **108** 063914

[7] Challa V.R. and Arnold D.P., MEMS Electrodynamic Vibrational Energy Harvesters using Multi-Pole Magnetic Architectures, *PowerMEMS 2012 (Atlanta, USA, 2-5 December 2012)*, concurrent publication.

[8] Zhu D., Beeby S.P., Tudor M.J., and Harris N.R., Vibration Energy Harvester Using the Halbach Array, *Smart Materials and Structures*, **21** 075020

[9] Peterson B.A., Herrault F., Oniku O.D., Kaufman Z.A., Arnold D.P., and Allen M.G., Assessment of Laser-Induced Damage in Laser-Micromachined Rare-Earth Permanent Magnets, *IEEE Trans. On Magnetics*, in press.